

Comparing the bulk radiated power efficiency in carbon and ITER-like-wall environments in JET.

P. Devynck¹, G. Maddison², C. Giroud², P. Jacquet², M. Lehnen³, E. Lerche⁴, G.F. Matthews², R. Neu⁵, M.F. Stamp², D. Van Eester⁴ and JET-EFDA Contributors*

JET-EFDA, Culham Science Centre, Abingdon, OX14 3DB, UK

¹CEA-IRFM F-13108 Saint-Paul-lez-Durance, France, ²CCFE Culham Science Centre, Abingdon, OX14 3DB, UK, ³ ITER Organization, 13115 Saint Paul-lez-Durance, France, ⁴ERM-KRS 1000, Brussels, Belgium, ⁵Max-Planck-Institut für Plasmaphysik D-85748 Garching, Germany

Abstract

We use a parameter β_r for all plasmas that allows detecting the pollution of the plasma bulk by highly radiative impurities. This parameter is defined as the radiative loss of the mixture of impurities relative to their mean Z^2 and was used in previous works to characterize the efficiency of radiative mantles in Neon seeded discharges [1,2]. We show that this parameter, though global, is very sensitive to the presence of highly radiative impurities in the bulk of the discharge. We use it to compare JET plasmas in the carbon environment and in the ITER-like wall (ILW), where it is highly correlated to the level of a bundle of spectroscopic lines of tungsten passing through the center of the discharge. In the carbon environment, the value of β_r is around 10^{-40} MW.m⁶, indicating the absence of highly radiative impurities in the plasma. No change or even a small decrease is observed when going from L-mode to H-mode, this robustness being in agreement with the multi-machine scaling [3]. In the ILW machine, the value of β_r is found to depend on the type of additional heating and confinement state of the plasma. We observe that neutral-beam injection (NBI) introduces little W into the plasma, with a β_r between 2 and 3 10^{-40} MW.m⁶. Ion-cyclotron radio-frequency (ICRF) waves yield a β_r of order 5 in L-mode and 10 10^{-40} MW.m⁶ in H-mode when no edge-localized modes (ELMs) are present. Conversely when ELMs are present, the parameter goes back to 5 10^{-40} MW.m⁶, illustrating the positive effect they can have on the bulk pollution by tungsten.

1) Introduction

Currently tungsten is being investigated as the preferred future material for tokamak divertors as its use solves several problems:

Firstly fuel retention should be minimized by the use of tungsten [4,5]. Another positive aspect is that tungsten is eroded at higher plasma temperatures than carbon [6]. At the moment it is being tested in a number of tokamaks [7] and is envisaged as the primary material for the divertor of ITER. However, apart from these qualities, there are some difficulties to operate machines with this type of high-Z material, in particular because it can

*See the Appendix of F. Romanelli et al., Proceedings of the 24th IAEA Fusion Energy Conference 2012, San Diego, US

radiate in the plasma core [8,9]. The presence of radiation in the centre of the discharge is a major concern for fusion machines and efforts are being made in present experiments to identify the radiating impurities in the core and estimate their concentration [10,11].

Spectrometers used for this purpose cover only lines or bundles of lines of these high-Z impurities along a few lines-of-sight and it is difficult from these measurements to deduce their concentrations. This can be done, in principle, with the help of radiation models which calculate the ionization equilibrium and which must include also the transport of the impurities. For high-Z elements, however, even the best of these models are only approximate. The case of tungsten is particularly difficult since many coefficients of radiative transitions in the highest ionization states are presently unknown.

As a result any information that can be gained about the radiative efficiency of the impurities polluting the bulk can be useful. This paper is a step in that direction. We analyze data from JET in its ITER-like wall (ILW) configuration [12] with tungsten divertor and beryllium torus walls and compare it with similar data from the earlier carbon environment.

We show that even global parameters can carry useful information about the type of impurities polluting the bulk of the discharge. In order to do this, we use a parameter defined in previous works [1,2] as the quality of impurity cooling. We show that this parameter is in fact the radiative loss parameter of the mixture of impurities relative to the square of their mean charge. The value and the changes of this parameter (called β_r) indicate a change of the impurity mixture and the pollution of the plasma by highly radiative species becomes immediately visible regardless of the level of the bulk radiated power.

In section 2 we write β_r as a function of P_{radbulk} , Z_{eff} and n_e and give its units. In section 3, the physical meaning of β_r is discussed in the light of the “radiative loss parameter” of the impurities as defined in reference [13]. In section 4, we discuss the filtering and influence of ELMs on determination of this parameter. Section 5 is dedicated to carbon-environment plasmas where we observe the changes in the β_r parameter from L to H mode. Section 6 is dedicated to the results obtained in the ILW environment. In 6.a we monitor first the different effects of NBI and ICRF waves on β_r in L-mode plasmas. In 6.b and 6.c we observe the L-H transition both for pure NBI and ICRF plasmas. In 6.d, we observe the correlation of β_r with the spectroscopic lines of high-Z impurities and discuss the effect of tungsten events on the evolution of the parameter. In section 7 we discuss how the different values of β_r affect the validity of the multi-machine scaling. We finish in section 8 with the conclusions.

2) The definition of β_r .

Following references [1,2] a parameter characterizing the quality of cooling of the impurities in the bulk of the plasma can be written as:

$$\beta_r = P_{\text{radbulk}} / (Z_{\text{eff}} - 1) n_e^2 \quad (1)$$

where n_e is the line-averaged density provided by high-resolution Thomson scattering [14] and Z_{eff} is calculated from bremsstrahlung emission [15] measured along a horizontal line-of-sight crossing the plasma centre (i.e. not passing through the divertor region). P_{rad} in the bulk is evaluated by bolometry, on JET using its most recent cameras (KB5) [16]. In order to estimate the bulk radiated power, only bolometric horizontal lines-of-sight in the top half of

the plasma are used to avoid the divertor region. The volume covered by them is then stretched to fill the whole plasma volume. In JET, we neglect the bremsstrahlung and cyclotron radiation; however, in a machine such as ITER, they will significantly contribute to the total radiated power and will have to be calculated or measured and removed from the total radiated power before evaluating β_r .

We give the expression for β_r in a general case where different types of impurities with different ionization levels are present in a deuterium plasma.

Firstly, for only one type of impurity, the radiated power (W) in the bulk may be written as:

$$P_{\text{radbulk}} = n_e n_{\text{imp}} V \sum_i a_i b_i c_i L_{ti} .$$

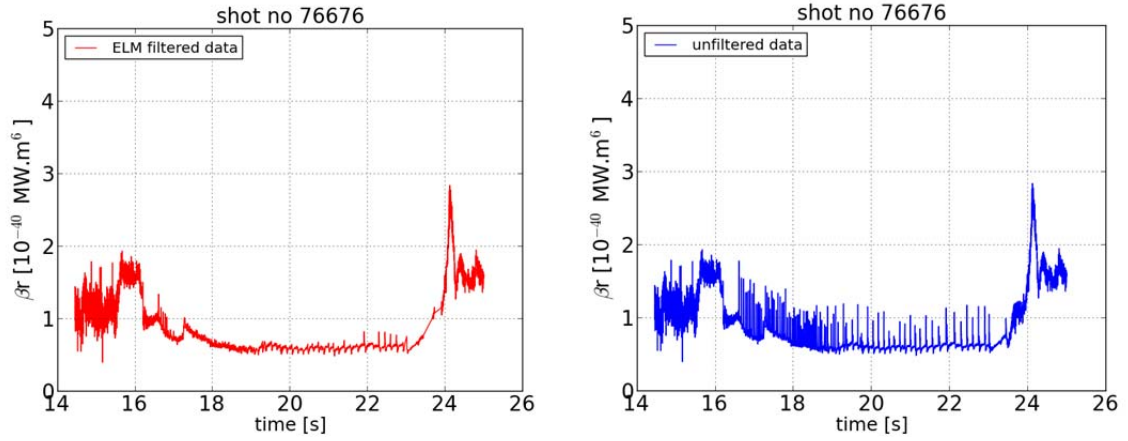


Figure 1

Shot 76676, carbon environment . H-mode, 12MW NBI heating. The result displayed is for the NBI heating phase only.

Left) β_r determined with ELM-filtered data. Right) β_r determined with unfiltered data.

In this expression n_{imp} is the total impurity density, n_e the electron density, $a_i = n_i / n_{\text{imp}}$ the fraction of impurity ions with charge Z_i , $b_i = n_{ei} / n_e$, the fraction of the density in the volume where the ion with charge Z_i radiates and $c_i = V_i / V$ the fraction of the volume in which the same ion radiates. L_{ti} is the radiative cooling function for the same ion with charge Z_i . We suppose in this expression that the electron temperature T_e is homogenous in the volume where the ion of charge Z_i is radiating, as well as the density of impurity ions and electrons. This is only an approximation. If we extend this to multiple impurities we get:

$$P_{\text{radbulk}} = n_e V \sum_k n_{\text{imp}}^k \sum_i a_i^k b_i^k c_i^k L_{ti}^k ,$$

where k denotes different types of impurities. We can write the expression for Z_{eff} as:

$$Z_{\text{eff}} = 1 + \frac{1}{n_e} \sum_k n_{\text{imp}}^k \sum_i a_i^k Z_i^k (Z_i^k - 1) .$$

If we combine these expressions in relation (1), we find

$$\frac{\beta_r}{V} = \frac{\sum_k \varepsilon_{\text{imp}}^k \sum_i a_i^k b_i^k c_i^k L_{ti}^k}{\sum_k \varepsilon_{\text{imp}}^k \sum_i a_i^k Z_i^k (Z_i^k - 1)} \quad (2) \quad \text{where } \varepsilon_{\text{imp}}^k = \frac{n_{\text{imp}}^k}{\sum_k n_{\text{imp}}^k}.$$

We notice that β_r/V is not dimensionless; it has the dimension of L_t and can be expressed in W.m^3 .

3) The physical meaning of β_r

The radiative loss parameter of an impurity k is defined in reference [13] as $S_k = \hat{P}_{\text{rad}k} / (n_e n_k)$, where \hat{P}_{rad} is radiated power density (W/m^3). It can be calculated using the same notations used in section 2.

We find in this case that for an impurity k , $S_k \approx \sum_i a_i^k b_i^k c_i^k L_{ti}^k$ where i takes account of the different ionization states.

Hence β_r can be expressed as a function of the radiative loss parameter of the impurities as:

$$\frac{\beta_r}{V} \approx \frac{\sum_k \varepsilon_{\text{imp}}^k S_k}{\sum_k \varepsilon_{\text{imp}}^k \sum_i a_i^k Z_i^k (Z_i^k - 1)}. \quad (3)$$

β_r is the weighted sum of the radiative loss parameters of the different impurities divided by the weighted sum of their average Z^2 . In reference [13], S_k has been calculated for different types of impurities in the bulk of the ASDEX Upgrade plasma using a coronal model. The coronal approximation can be used if the residence time of the impurities in the plasma is

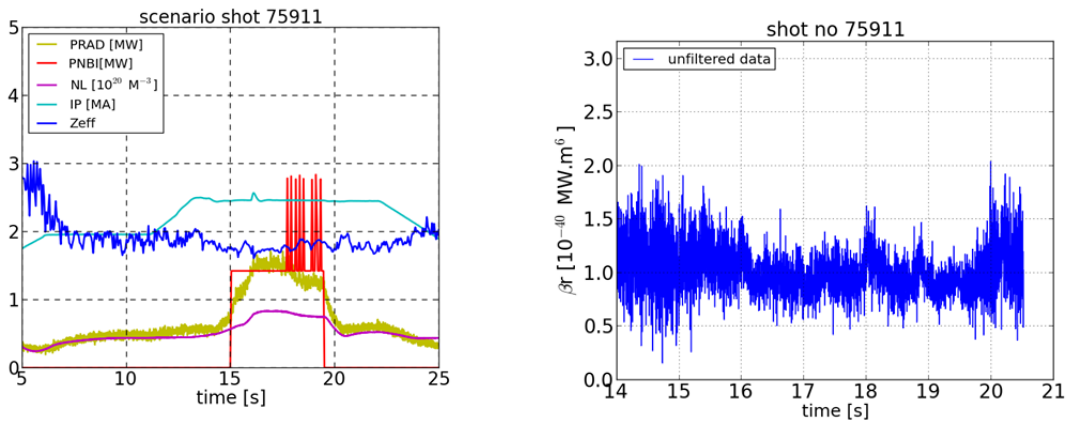


Figure 2

Left : scenario for shot 75911, L-mode, **carbon environment** , NBI from 1.4 to 2.8 MW

Right: β_r calculated during the NBI heating phase.

sufficiently long and the plasma in steady state. These conditions can be encountered in the plasma bulk in contrast to the SOL and divertor region where the residence time of the impurities is too short. The result does not depend strongly on the plasma density as long as multi-step processes are weak. If we take the two main impurities for the JET shots (carbon

for the carbon divertor and tungsten for the ILW configuration), the results shown in Figure 1b of reference [13] show that the S_W for tungsten has a value of order 10^{-31} Wm^3 while it is less than 10^{-34} Wm^3 for carbon. For W, the radiative loss parameter increases moderately for T_e above 100 eV (about a factor of 2 between 100 eV and 3 keV), while it decreases by a factor of 10 for carbon in the same range. Tungsten is at least 3 orders of magnitude more efficient at radiating in the bulk than carbon. This is the well-known result that a tiny fraction of tungsten ($\sim 10^{-4}$) can drive a large radiation loss in the bulk.

The changes of β_r may be discussed using the dependence of the radiative loss parameter with T_e discussed above. In the case of W pollution, the rather weak dependence of S_W with T_e leads to the conclusion that an increase of β_r must be associated with an increase of the relative concentration of W in the bulk $\varepsilon_{\text{imp}}^W$ (even if this increase is not sufficient to have a measurable impact on Z_{eff}). The second point is that the value of β_r is liable to be very resilient to T_e changes with tungsten pollution. A decrease of β_r can have different causes. It can be triggered by an increase of low Z impurities that have a very small radiative loss parameter (increase of Z_{eff} and of the denominator in relation (2)), or a decrease of the fraction of tungsten impurities $\varepsilon_{\text{imp}}^W$ (no or small change in Z_{eff}), or a combination of these two processes, as is occurring during impurity seeding, for example. Finally, in the ILW changes in the values of β_r will always indicate a change in the bulk impurity mixture.

4) Experimental determination of β_r , filtering

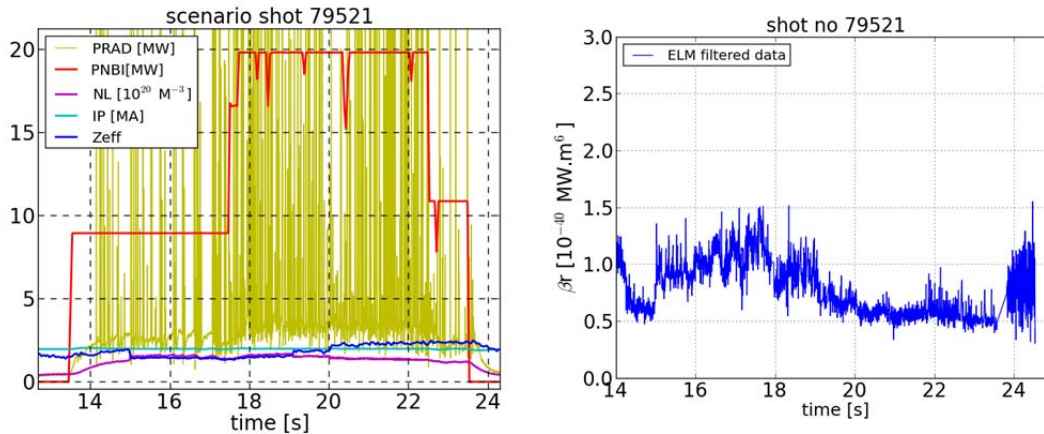


Figure 3

Left) scenario of shot 79521, carbon **environment**.
Right) β_r calculated during the NBI additional heating phase.

β_r can be simply calculated as:

$$\beta_r(t) = \frac{P_{\text{radbulk}}(t)}{(Z_{\text{eff}}(t) - 1)n_e^2(t)}.$$

The value of β_r is interesting to follow during plasma shot to check rapidly if the mixture of impurities contaminating the bulk evolves. However strong events such as ELMs [17] may

affect relation (1) or even break it, so that it is in principle necessary to filter the data to

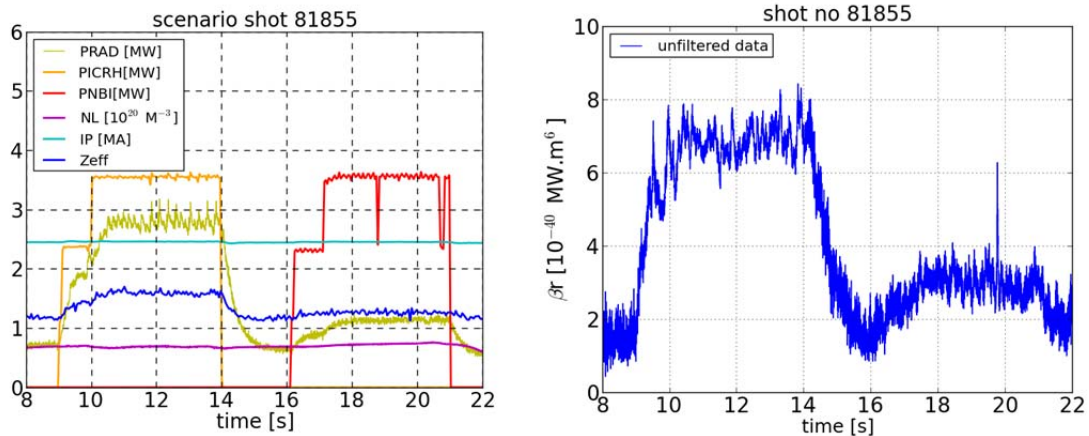


Figure 4

Left) scenario of shot 81855, L-mode, ICRF then NBI heating.

Right) value of β_r calculated during the additional heating phases.

remove these non-stationary phases before computing β_r. However we show that from an operational point of view, β_r can be calculated without filtering. There are two reasons for this: $P_{\text{rad bulk}}$ is quite insensitive to ELMs that are edge phenomena, and Z_{eff} and n_e are line-averaged quantities rather resilient to edge changes. In order to illustrate this, we show in Figure 1 β_r(*t*) calculated for a 12 MW NBI H-mode shot with very large Type I ELMS where first a histogram filtering is applied on the ELMs (Fig.1, left) and second without ELM filtering (Fig.1, right). This comparison shows that even without filtering, the value of β_r can be reliably recovered and followed in time.

5) Carbon environment L and H-mode.

The results which we present are selected from the whole JET database and several thousand shots have been scanned automatically. Although only the results from a few shots are presented here, they do represent very well the behavior of the whole data base. In Figure 2 β_r is plotted for an L-mode shot with low NBI power (1.4 MW). It is found to be very close to 1 throughout the heating phase. In Figure 3, the same parameter is plotted for an H-mode shot with ELMs. Two heating phases are present, the first with 9 MW of NBI power, the second with 19 MW of NBI power. Figure 3 shows that that the 9 MW phase has a value of β_r close to 10⁻⁴⁰ MW.m⁶ as in L-mode. At 19 MW, β_r decreases to 0.5 10⁻⁴⁰ MW.m⁶. This decrease may be attributed to the behavior of the radiative loss parameter of the light impurities and carbon (S_C) in particular. As the additional heating power is increased, T_e increases in the whole bulk including the pedestal region. As a consequence, the radiative loss parameter of carbon decreases (numerator of relation (2)), thus yielding lower β_r values. This simply indicates that the low-Z impurities become even less efficient at radiating in the bulk when T_e is increased. We notice that at NBI heating power below 10 MW, the β_r value is the same in L or H-mode. This shows how robust the value of the β_r parameter is in carbon discharges, an observation which partly explains the robustness of the multi-machine scaling [3].

6) ITER-like-wall environment

6.a Specific effects of ICRF and NBI heating in L-mode

In the carbon environment, wall and divertor surfaces are eroded by physical and chemical erosion but there are also specific interactions of the additional heating with the walls. In the ILW environment, these specific interactions with the wall and divertor structure are critical and the level of tungsten sent to the bulk of the discharge may depend on the type of additional heating. This is examined by comparing ICRF and NBI heating at same power during stationary L-mode conditions. The scenario of the shot plotted in Figure 4 shows that during ICRF heating Z_{eff} is larger than during NBI heating. This suggests that during ICRF more low-Z impurities are also released (such as Be) than during NBI heating, suggesting stronger interaction with the walls. However, the value of β_r is $7 \cdot 10^{-40} \text{ MW.m}^6$ during ICRF and $3 \cdot 10^{-40} \text{ MW.m}^6$ during NBI heating. This clearly shows that during ICRF the bulk plasma is more polluted by highly radiative impurities than during NBI operation.

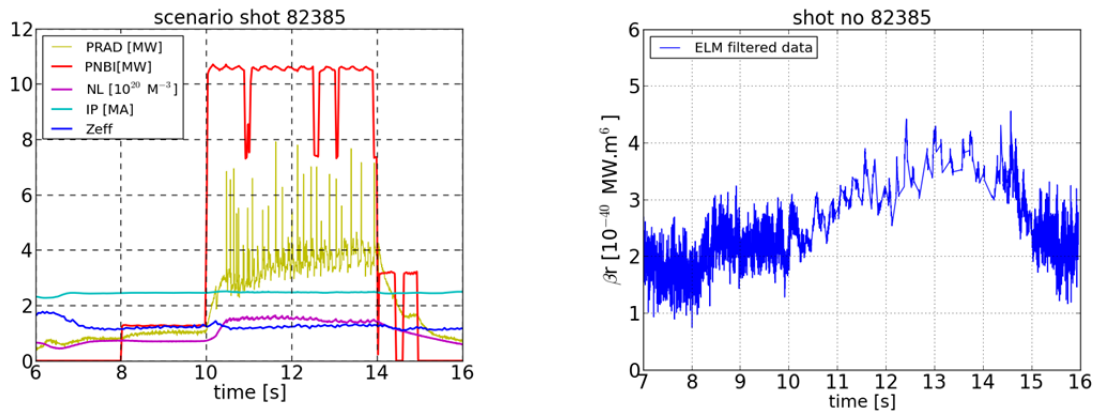


Figure 5

Left) scenario of shot 82385, L-H transition, NBI heating.

Right) value of β_r calculated during the additional heating phases.

If we compare these results with those obtained in the carbon environment, we see that during NBI heating in the ILW, the lowest value of β_r is somewhere between 2 and $3 \cdot 10^{-40} \text{ MW.m}^6$, while the average value in carbon is 10^{-40} MW.m^6 . This higher value suggests that even with NBI heating some small amount of tungsten is nevertheless added to the bulk.

6.b ILW transition from L- to H-mode with NBI only.

Figure 5 illustrates the behavior of β_r when there is an L-H transition with NBI heating. We notice first that the value of β_r during the L-mode phase ($8\text{s} < t < 10\text{s}$) is lower than that measured in L mode in the shot above (#81855), 2.2 instead of $3 \cdot 10^{-40} \text{ MW.m}^6$. The pollution of the plasma by high-Z impurities depends on its history and using NBI after ICRF is less favorable than operating with NBI heating only. We have measured values as low as $1.3 \cdot 10^{-40} \text{ MW.m}^6$ for some ILW plasmas during NBI heating, close to those measured in carbon pulses. During the H-mode phase ($10\text{s} < t < 14\text{s}$), β_r increases from 2.2 to an average $3.7 \cdot 10^{-40} \text{ MW.m}^6$, a 68% increase, though the additional heating power is increased from 1.5 MW to 10 MW. This result illustrates the fact that in this scenario, NBI heating increases moderately the amount of

high-Z impurities from L to H-mode. The fact that Z_{eff} remains unchanged also indicates that the pollution by low-Z impurities does not increase either.

6.c ILW transition from L to H-mode with ICRF only

In Figure 6, a plasma where only ICRF is used triggers an L-H transition. This is visible in the plasma traces where the D_{α} signal drops at $t=17.27\text{s}$. The energy stored in the discharge is not sufficient to trigger ELMs. This type of shot has been studied and reported in [18]. After the transition, β_r increases from 5 to 10, a 100% increase. β_r around $10^{-39} \text{ MW}\cdot\text{m}^6$ is the

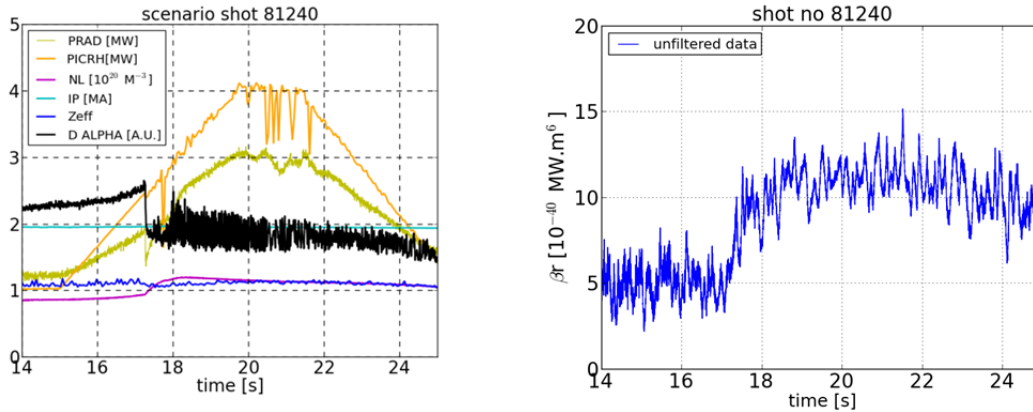


Figure 6

Left) scenario of shot 81240, L- H mode transition , ICRF heating.

Right) value of β_r calculated during the additional heating phases.

level commonly observed in the JET database when ICRF triggers H-modes without ELMs. It is one of the highest values obtained so far for β_r . As the level of β_r jumps to $10^{-39} \text{ MW}\cdot\text{m}^6$ immediately after the ICRF power has reached the threshold, it can be speculated that this is partly the effect of the transport change. As transport decreases in the bulk after the H transition, the amount of impurities there increases. There are other indications of fluctuation effects on β_r when ICRF power is being used. For example, when ELMs are present in the discharge, a combination of NBI and ICRF heating power produces β_r values of order only $5 \cdot 10^{-40} \text{ MW}\cdot\text{m}^6$. Once the NBI is decreased and the ELMs disappear, β_r reverts to $10^{-39} \text{ MW}\cdot\text{m}^6$. This illustrates the beneficial effect of ELMs for ejection of impurities from the bulk.

6.d Linkage of β_r with impurity lines measured in the discharge.

β_r is the radiative loss parameter of the mixture of impurities polluting the bulk relative to its mean Z^2 . As the radiative loss functions of the impurities scale roughly as the cube of their charge [13], the β_r values are extremely sensitive to the amount of highly radiative impurities such as tungsten in the discharge; thus β_r is a potent parameter to detect them. As a result it can be expected that β_r should be correlated with the spectroscopic lines of these highly radiative impurities [19]. This is indeed the case, as is shown in Figure 7. β_r is plotted as a function of time together with a bundle of tungsten lines emitted from the center and a line of nickel XVIII radiated at the edge of the bulk plasma. To facilitate comparison of the different

signals, they are normalized to the same scale. The data in Figure 7 show that β_r is extremely well correlated with the bundle of W lines between 8 and 9 s but shows no variation with the very large peak of nickel XVIII that occurs between 10 and 10.2 s. As a result, the increase of the bulk radiation at the beginning of the NBI heating phase where both tungsten and nickel lines are present (8 to 9 s) can be unambiguously attributed to emission by tungsten. Another point is that β_r can detect a pollution of the bulk plasma after a so-called tungsten event, i.e. a sudden large influx typically due to ingression of a dust grain or flake [20]. This is illustrated in Figure 8 which shows the variation of β_r during a time window where such an event occurs in a 9.4 MW NBI heated H-mode shot. The ELMs have not been filtered and are visible on the data. It is unclear at the moment the exact role they play in the recovery time of the radiation profile which exactly matches the recovery time of the β_r parameter. We note

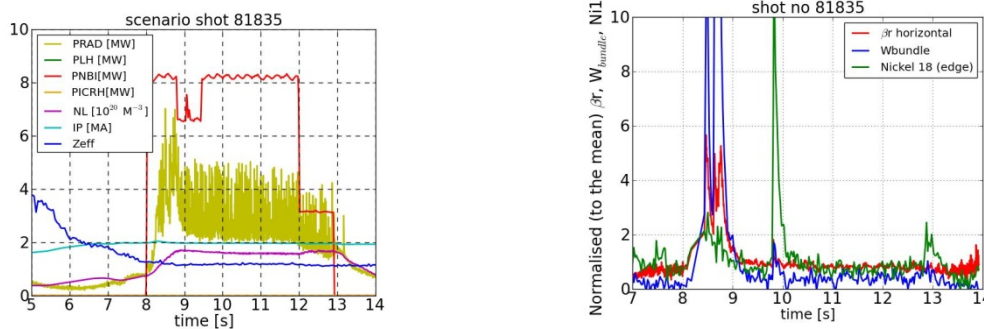


Figure 7

Left) scenario of shot 81835, H-mode transition, 8 MW of NBI heating.

Right) β_r , W line bundle and Ni XVIII line as a function of time during NBI phase. Data normalized to the same scale.

however a drop of the β_r parameter at 13.5s that corresponds to the crash of a very large ELM. Before the tungsten event, at 13.4s, β_r has a value of $2.6 \cdot 10^{-40} \text{ MW.m}^6$, then after the event at 13.7 s, it goes back to a value around $4 \cdot 10^{-40} \text{ MW.m}^6$, indicating that some tungsten has been added to the bulk of the discharge and is radiating there. This is confirmed by the bolometry data which show peaking of the radiation in the mid-plane on the low-field side of the plasma (the usual signature of tungsten radiation with NBI heating [21]) after the tungsten event. Notice also that before the tungsten event, the value of β_r was quite low and in agreement with that usually observed with NBI heating.

7) β_r and the the multi-machine scaling.

The multi-machine scaling of plasma purity with radiated power [3] was derived at a time when most of the tokomaks involved were equipped with carbon wall components. The most common impurity in the plasma apart from carbon was oxygen, which is another low-Z impurity also radiating at low T_e . The scaling was used to characterize the total radiated power (bulk and divertor) in a situation where it was dominated by the radiation of low-Z impurities. Such a situation implied that most of the time, the radiated power in the divertor was larger than that from the bulk. The simplified form of the multi-machine scaling reads as:

$$Z_{\text{eff}} \approx 1 + 7.5 \frac{P_{\text{rad}}^{\text{tot}}}{An_e^2} \quad (4)$$

where $P_{\text{rad}}^{\text{tot}}$ is the total radiated power and A the plasma envelope area.

First of all, the multi-machine scaling is not directly related to the value of β_r that we measure in the bulk of the discharge. This is because of the contribution of the divertor radiation to this scaling. We found in section 5 that β_r varies between 0.5 and 1.10^{-40} MW.m⁶ in carbon

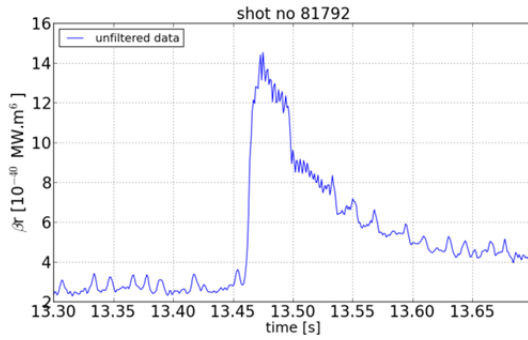


Figure 8
 β_r as a function of time during a tungsten event, shot 81792. H-mode, 9.5 MW NBI heating

environment. For this range of values, the multi machine scaling is verified with some dispersion. This is shown in Figure 9 where the Z_{eff} predicted by the scaling is plotted versus the Z_{eff} integrated along a vertical Line of Sight. The result plotted in Figure 9 is for the shot displayed in Figure 3. In this shot, the bulk and divertor radiated power are about at the same level. However, most of the dispersion of the data around the scaling observed in Figure 9

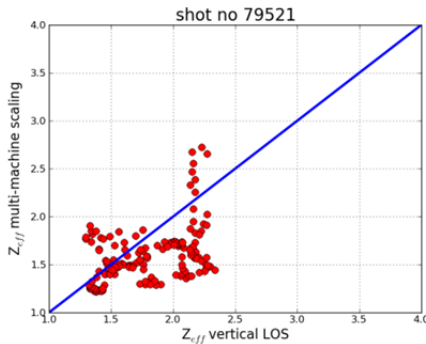


Figure 9
Test of the multi-machine scaling [3] using relation (4), shot 79521, carbon environment, H-mode, NBI heating phase.

comes from the contribution of the divertor radiation. This is a general result, we find that if most of the time the bulk radiation follows the generic form of the multi-machine scaling law very well (the points are well aligned i.e. β_r varies little), the divertor radiation has the correct order of magnitude to fit in the scaling but introduces some dispersion or even deviation from this scaling. This comes from the fact that the divertor radiation has less correlation with the changes of global parameters (like mean Ne and line integrated Z_{eff}) than the bulk radiated power.

In general, we find that for experimental values of $\beta_r < 4 \cdot 10^{-40}$ MW.m⁶, there is reasonable agreement of the data with the multi-machine scaling. For rising β_r values above $4 \cdot 10^{-40}$ MW.m⁶, the data depart increasingly from the multi-machine scaling.

In order to illustrate this, we plot in Figure 10 left the prediction of Z_{eff} by the multi-machine scaling as a function of Z_{eff} issued from the experiment. The shot is #81855 in ILW studied in section 6.a and plotted in Figure 4. The Z_{eff} predicted by the multi-machine scaling is systematically above the one calculated from experimental data. The difference between the

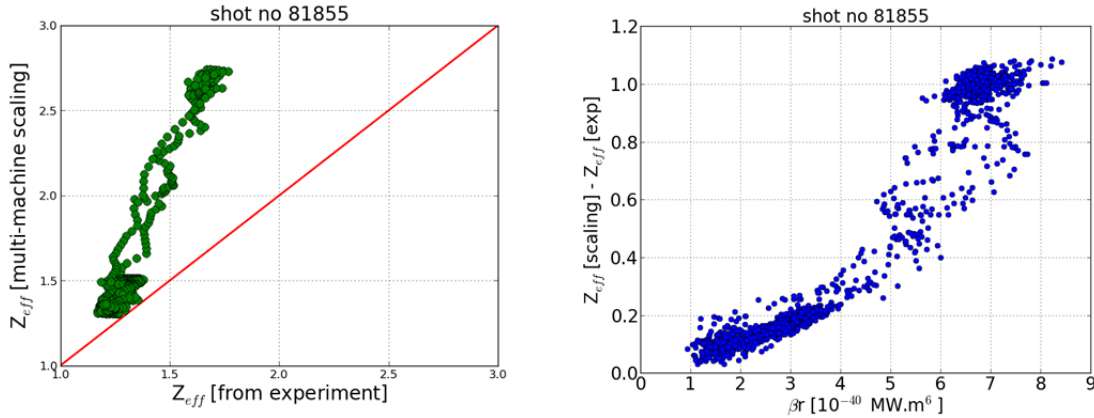


Figure 10

Left) shot 81855, ILW, ICRH and NBI heating, Z_{eff} predicted by multi-machine scaling as a function of Z_{eff} from experimental data (horizontal LOS Bremsstrahlung). Right) difference between Z_{eff} from multi-machine scaling and Z_{eff} from experimental data as a function of β_r .

Z_{eff} predicted by the scaling and the one issued from the experimental data is plotted as a function of β_r in Figure 10 right. The data with a β_r around 3 (NBI phase) has a Z_{eff} close to the one predicted by the multi-machine scaling but the data with β_r around 7 (ICRF phase) departs from the prediction of the scaling by about 1 (2.7 instead of 1.7). Figure 10 right clearly shows that the departure from the multi-machine scaling occurs with the increase of β_r i.e. when high Z impurity in the plasma bulk start to dominate the radiated power. Another way to measure the departure from the multi-machine scaling is to define a radiation enhancement factor:

$$D = \frac{P_{\text{rad}}^{\text{tot}}}{\left(\frac{A}{7.5}\right) (Z_{\text{eff}} - 1) N_e^2} \quad (5)$$

This enhancement factor is a dimensionless parameter that measures how much more radiative the discharge is, relative to the situation where the multi-machine scaling applies. We plot D for the shot 81855 in Figure 11 together with β_r . Although the two parameters measure different things (β_r measures the radiative efficiency of the bulk impurities relative to their mean Z^2 without reference to any scaling, D is an enhancement factor of the total radiated power relative to a scaling law) the behavior of the two parameters as a function of time is similar. Discharge #81855 is 2.5 five times more radiative than what predicted by the scaling during ICRF heating while it is only 1.5 more radiative than the scaling in the case of NBI heating. The comparison of the behavior of β_r and D in Figure 11 leads to the same conclusion than the one obtained from Figure 10 right: The deviation from the scaling comes from the radiation of high Z impurities in the bulk.

Finally all these results show that the multi-machine scaling corresponds to the lowest radiation state of the bulk plasma and does not apply when high-Z impurities start to dominate the radiation in that region.

8) Conclusions

We have shown that a global time-dependent parameter can give fast and reliable information about the presence of highly radiative impurities in tokamak discharges. It can be calculated for all plasmas regardless of the scenario and of the confinement state. We have compared JET shots in the carbon environment with ones in the ILW. The very low values obtained in the carbon environment clearly indicate the absence of significant radiation from highly radiative impurities in the bulk plasma, with an average value of $\beta_r \approx 10^{-40} \text{ MW.m}^6$. One of the striking results in carbon is that the variation of β_r with the plasma scenarios is small. This

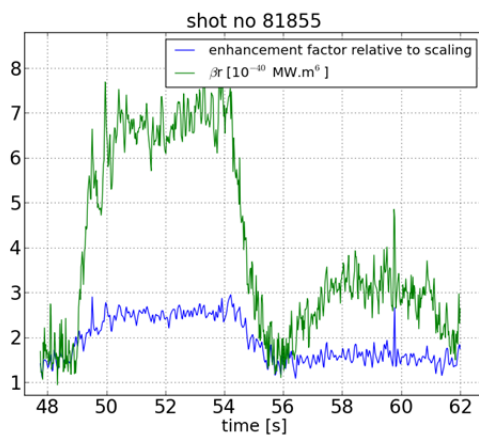


Figure 11

Shot 81855, ILW, ICRH then NBI heating. D radiation enhancement factor and β_r as a function of time.

result and the lack of high Z impurities in the bulk partly explain the robustness of the multi-machine scaling [3] that applies to carbon-dominated plasmas and proposes a constant coefficient of the scaling for each machine. When switching to the ILW environment, we observe that β_r increases above 10^{-40} MW.m^6 , this increase being clearly dependent on the plasma scenario: viz. the confinement mode, the fuelling of the plasma, and the type of additional heating used. By comparing the effect of the different types of additional heating, we observe that plasmas heated with NBI have relatively low β_r values of order 2 to 3 times those measured in the carbon environment. This indicates that NBI heating sends little tungsten into the bulk. During the L-H transition the β_r parameter is observed to increase moderately even with a sevenfold increase of the NBI power. This situation compares well with the carbon environment and confirms lower pollution by tungsten. We notice however that even with this type of additional heating, tungsten emission events do occur and can lead (in the case of strong events) to pollution of the core by additional tungsten. β_r is strongly correlated to the bundle of W lines measured in the centre of the discharge but can still detect W pollution even when the radiation is displaced out of the spectroscopic lines-of-sight. In the case of ICRF heating, these plasmas systematically yield β_r values of order $5 \cdot 10^{-40} \text{ MW.m}^6$ in L-mode and 10^{-39} MW.m^6 in H-mode if no ELMs are present. In the presence of ELMs, β_r values are reduced back to a value of $5 \cdot 10^{-40} \text{ MW.m}^6$, illustrating very well the beneficial effect of ELMs on W pollution. In the ILW, we have not observed so far (experimental campaigns 2011, 2012, 2013) values of β_r below $4 \cdot 10^{-40} \text{ MW.m}^6$ when ICRF

power is being used to heat the plasma. These values are extremely robust over the entire database and clearly indicate that ICRF introduces more tungsten in the discharge than NBI heating.

Finally β_r is a global parameter that is not straightforward but it has some advantages: it is extremely sensitive to the pollution of the plasma by highly radiative impurities and can detect them when no other diagnostic is available. It has also the virtue of being easily calculated with standard measurements and can be determined even without ELM filtering. Its time evolution can be followed during a shot and provides quantitative values which can be compared from shot to shot. For these reasons, it could be useful for many machines, including ITER.

Acknowledgments:

This work was supported by EURATOM and carried out within the framework of the European Fusion Development Agreement. The views and opinions expressed herein do not necessarily reflect those of the European Commission

References

- [1] G. Telesca et al, Nucl. Fusion, **40**, No. 11,1845
- [2] L. Carraro et al., Nucl. Fusion, **40** (2000), No. 12, 1983
- [3] G.F. Matthews et al., J. Nucl. Mater. 241-243 (1997) 450
- [4] V. Rohde et al., Nucl. Fusion **49** (2009) 085031
- [5] T. Loarer, Journal of Nuclear Materials 390–391 (2009) 20–28
- [6] C.H. Wu, U. Mszanowski, Journal of Nuclear Materials 218 (1995))
- [7] A. Kallenbach et al 2009 Nucl. Fusion **49** 045007
- [8] R. Neu et al, Journal of Nuclear Materials 313–316 (2003) 116–126
- [9] J.C. Fuchs et al., 35th EPS Conference on Plasma Phys. Hersonissos, 9 - 13 June 2008 ECA Vol.32D, P-2.012 (2008)
- [10] T. Pütterich et al. 2012 Proc. 24rd IAEA Fusion Energy Conf. (san Diego,CA) (Vienna: IAEA) vol. IAEA-CN-197, EX-P3.15
- [11] T. Pütterich et al., Plasm. Phys. Control. Fusion 55 (2013) 124036.
- [12] G.F. Matthews, Phys. Scr. T145 (2011) 014001
- [13] R. Neu et al, 2010 proc. 24rd IAEA Fusion Energy Conf. (Daejon,Rep. of Korea),vol.IAEA-CN-180, EX/D-P3-24.
- [14] R. Pasqualotto et al., Rev. Sci. Instrum. **75**, 3891 (2004)
- [15] H. Meister et al, Rev. Sci. Instrum. **75**, 4097 (2004)
- [16] A. Huber et al., Fusion Engineering and Design 82 (2007) 1327.
- [17] A. Loarte et al, Plasma Phys. Control. Fusion **44** (2002) 1815–1844
- [18] C.F. Maggi et al., 39th EPS Conf. on Plasma Physics (Stockholm) 2012.
- [19] Czarnecka et al., Plasma Physics and Controlled Fusion 53, 035009 (2011)
- [20] J.W. Coenen et al., Nucl. Fusion **53** (2013) 073043 .
- [21] E. Joffrin et al. Nucl. Fusion **54** (2014) 013011.